**7th International Symposium on Superalloy 718 and Derivatives**
*Edited by: E.A. Ott, J.R. Groh, A. Banik, I. Dempster, T.P. Gabb, R. Helmink, X. Liu, A. Mitchell, G.P. Sjöberg, and A. Wusatowska-Sarnek*
***TMS (The Minerals, Metals & Materials Society), 2010***

# FE SIMULATION OF MICROSTRUCTURE EVOLUTION DURING RING ROLLING PROCESS OF INCONEL ALLOY 783

Jong-Taek Yeom[1], Eun-Jeoung Jung[1], Jeoung Han Kim[1], Jae-Keun Hong[1], Nho-Kwang Park[1], Kook-Joo Kim[2], Jin-Mo Lee[2], Seung-Sik Choi[2]

[1]Korea Institute of Materials Science (KIMS); 66 Sangnam-Dong; Changwon, 641-831, Korea
[2]Taewoong Co.; 1462-1 Songjeong-Dong; Gangseo-gu, Busan, 618-270, Korea

Keywords: INCONEL Alloy 783, Microstructure Evolution, Recrystallization, Ring Rolling

## Abstract

In this study, microstructure evolution during ring rolling process of INCONEL alloy 783 (Alloy 783) was investigated with the combined approaches of 3-D FEM (Finite Element Method) simulation and microstructure prediction model. A microstructure prediction model was developed by considering the effects of process variables on recrystallization and grain growth behavior. The model was established by the analysis of hot compression and isothermal heat treatment test results. From the analysis of isothermal heat treatment tests, it can be found that the rate of grain growth dramatically increases after the dissolution of β phase, which acts as an obstacle to grain boundary movement. In order to consider the effect of β phase on grain growth, an additional equation in the transition temperature region was interposed. Microstructure evolution during ring rolling process of Alloy 783 was calculated by de-coupled approach between FEM analysis and microstructure prediction model. The prediction results were compared with the experimental ones.

## Introduction

INCONEL alloy 783 (Alloy 783) is an oxidation-resistant, low expansion, nickel-cobalt-iron alloy with aluminium, chromium, and niobium additions [1]. The mechanical properties of Alloy 783 depend very much on grain size and the strengthening phases, γ′($Ni_3Al$-type) and β (NiAl-type). Especially, grain size control in the hot working processes of this alloy is an important issue in pursing integrity of structure and properties. For instance, a fine grain size structure has high strength and good low-cycle fatigue properties while a larger grain size structure indicates good creep and defect tolerance properties. The grain size change of Alloy 783 during hot forming and heating is mainly controlled by the recrystallizaton and grain growth behaviours. The recrystallization behaviour is influenced by process variables such as the forming temperature, strain rate, initial grain size and amount of deformation [2]. Generally, the kinetics of recrystallization and grain growth processes are complex. In order to control the grain size distribution during high temperature deformation, a basic understanding of the microstructure evolution during complex manufacturing sequences, including heating, soaking and hot working, should be made as an essential prerequisite.

In this work, a microstructure prediction model is implemented into a commercial FE code based on the analytical understanding of the microstructural change in Alloy 783 during high temperature deformation. Constitutive model considering dynamic recrystallization and grain growth theories was used for the prediction of grain structure in ring-rolled Alloy 783 ring. Model parameters were determined by the isothermal heat treatment and hot compression tests.

Finally, the simulation results were validated by comparing the experimental observation for a large-scale Alloy 783 ring manufactured by ring rolling process.

## Experimental Procedures

### Material

The material used in this work was the forged Alloy 783 billet. The chemical composition of is given in Table I.

Table I. Chemical compositions of the as-received Alloy 783 billet. (wt.%)

| C | Mn | Fe | S | Si | Cu | Cr | Al | Ti | Co | Nb | Ta | P | N |
|---|---|---|---|---|---|---|---|---|---|---|---|---|---|
| 0.01 | 0.03 | 24.9 | 0.001 | 0.06 | 0.04 | 3.28 | 5.36 | 0.2 | 34.8 | 2.99 | 0.006 | 0.005 | Bal. |

Alloy 783 is a Ni-Fe-Co base superalloy containing $\gamma'$ ($Ni_3Al$-type) and $\beta$ (NiAl-type) phases in $\gamma$ austenite matrix. The average grain size of the alloy was ASTM # 6.5~7.5 (~33.1μm), as shown in figure 1.

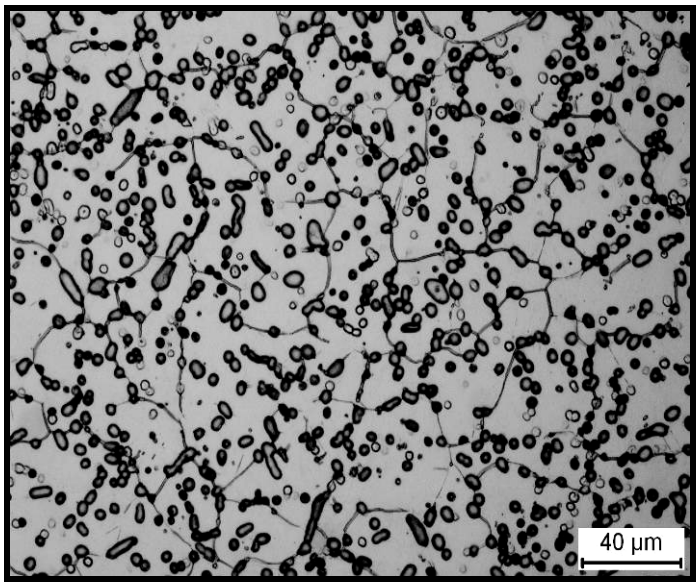

Figure 1. Microstructure of as-received Alloy 783 alloy billet

### Hot Compression and Isothermal Heat Treatment Tests

In order to investigate the deformation behaviour and microstructural evolution during high temperature deformation, compression tests on cylindrical Alloy 783 with 8mm in diameter and 12mm in height were carried out at the temperature range between 800°C and 1200°C at 50°C intervals and at strain rates varying from $10^{-3}$ - $10s^{-1}$. Test specimens were induction heated to test temperatures at a heating rate or cooling rate of 5°C/s and held constant for 5min at the same temperatures to secure temperature uniformity in the samples. All the tests were performed in vacuum ($10^{-2}$ Torr) using a computer-controlled servo-hydraulic testing machine. Tantalum foil of 0.1mm thickness was used between the specimen and anvils to avoid sticking of the specimen to the anvils. To observe the evolution of microstructure during compression tests, the compression-tested specimens were quenched soon after the compression tests with $N_2$ gas to freeze the microstructures. In order to analyze the grain growth behaviour of Alloy 783,

isothermal heat treatment tests were carried out for the different hold times between 950 and 1200°C, and the tested samples were quenched by water.

Simulation and Ring Rolling Process

To simulate the effect of process variables such as strain, strain rate and temperature on the grain size distribution of the samples, a commercial finite element (FE) code, SHAPE-RR, was used for the simulation of ring rolling process. Post user-subroutine for microstructure model based on recrystallization and grain growth theories was used to predict the grain size distribution during ring rolling process. Alloy 783 ring with the outer diameter of approximately 740mm was manufactured by ring-rolling process. The ring rolling equipment used in this work has the manufacturing capacity of outer diameter in the maximum 3,000mm and the maximum rolling force of about 100ton. Angular velocity of the main roll and average feed rate of the mandrel were applied as 26rpm and 0.5mm/s, respectively. The preform (or blank) temperature for the ring rolling was 1100°C. After the ring rolling, Alloy 783 ring was water-quenched.

## Results and Discussion

Strain and Stress Curves of Alloy 783

The typical flow behaviours obtained from hot compression tests with various test conditions are presented in Figure 2. The shape of the flow curves depends on the strain rate and temperature. In the flow curves, the initial work hardening rate decreases continuously with strain, and the flow curve reaches essentially a peak stress. Afterwards, the curve decreases to a steady state stress level. In general, the softening of the curve can be attributed to adiabatic deformation heating and dynamic recrystallization.

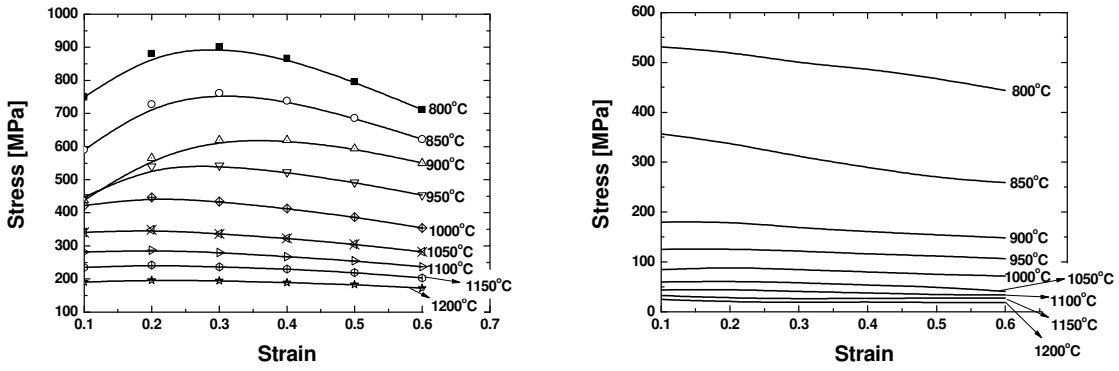


(a) Strain rate =10$s^{-1}$ (b) strain rate = $10^{-3}s^{-1}$

Figure 2. Typical flow stress curves of Alloy 783 obtained from hot compression tests

In order to clarify the flow softening effect in flow curves, the flow stress curves were corrected for the deformation heating effects using the following expression [3].

$$\Delta T = \frac{\psi \int_0^{\bar{\varepsilon}} \bar{\sigma} d\bar{\varepsilon}}{C_p \rho} \tag{1}$$

where $\psi$ is the fraction of plastic work converted to heat, taken here to be 0.9. $\rho$ is density, $C_p$ is heat capacity. The flow curves are then plotted against $T_0+\Delta T$, where $T_0$ is the nominal test temperature and the isothermal flow stress data are obtained by interpolation from these plots. Also, the microstructures corresponding to truly isothermal deformation at $T_0$ was utilized for generating the material parameters of the model.

Microstructure Prediction Models

As a constitutive model for description of flow stress at high temperature, the most common approach is based on the hyperbolic sine function relationship between flow stress and deformation rate originally introduced by Garafalo [4]. Also, the strain rate and temperature dependence of the flow stress can be expressed by Zener-Hollomon parameter, Z. The relationship between the hyperbolic sine function and Z can be expressed by the following equation.

$$\dot{\varepsilon} \cdot \exp(-Q / RT) = A \cdot [\sinh(\alpha \cdot \sigma_{\max})]^n = Z \tag{2}$$

where Q is a pseudo activation energy, T is the absolute temperature and R is the universal gas constant. The values including the constitutive equation can be determined by a least square method. The values of $\alpha$, Q, A, and n were 0.0085, 575kJ/mole, $3.272 \times 10^{20}$ and 2.9, respectively.

The critical strain is an important measure for the onset of dynamic recrystallization. The critical strain is determined by the strain that corresponds to the critical stress($\sigma_c$) indicating the sudden drop of the hardening rate ($\theta=d\sigma/d\varepsilon$) in the strain hardening rate, $\theta$ vs. $\sigma$ plots. A more detailed discussion of the determination of the critical strain is presented elsewhere [5]. The equations developed for the critical strain are expressed as a function of Zener-Hollomon parameter, Z. For Alloy 783, the equation of critical strain is as follows:

$$\varepsilon_c = 7.032 \times 10^{-5} \cdot Z^{0.128} \tag{3}$$

In general, the dynamic recrystallization progresses in a sigmoidal manner with respect to strain. The relationship between the fraction of dynamic recrystallization and strain can be expressed by the Avrami equation.

$$X = 1 - \exp(-\ln 2(\varepsilon / \varepsilon_{0.5})^n) \tag{4}$$

The strain for 50% recrysatllization, $\varepsilon_{0.5}$ can be determined by microstructure analysis results of compression tests with different magnitudes of strain for a given condition of temperature, strain rate and starting grain size. The strain for 50% recrystallization, $\varepsilon_{0.5}$ for Alloy 783 is given by the following equation.

$$\varepsilon_{0.5} = 5.723 \times 10^{-10} \cdot \dot{\varepsilon}^{0.085} \cdot \exp\left(\frac{2.93 \times 10^4}{T}\right) \tag{5}$$

Also, best fits to the exponential coefficient n was 1.2.

The size of dynamically recrystallized grain is the function of Zener-Hollomon parameter, Z, only. This is because that when dynamic recrystallization reaches steady state the new grain occupies the entire space of the old grain. For Alloy 783, the relationship between dynamically recrystallized grain, $d_{drx}$ and Z is shown as follows:

$$d_{drx} = 4.73\times10^{5}\cdot Z^{-0.218}(\mu m) \tag{6}$$

Under preheating period or post heat treatment, grain growth happens as a function of time. Grain boundary energy is the driving force causing grain boundary motion at high temperature. The growth of grain size with increasing time can be obtained from the analysis results of isothermal heat treatment tests. From the analysis of isothermal heat treatment tests, it can be found that the rate of grain growth dramatically increase after the dissolution of beta phase (NiAl) acting as an obstacle against grain boundary movement. The change in grain size vs. time for Alloy 783 considering the β phase effect is found to follow relationship:

$$D_1^{2.3} = D_0^{2.3} + 3.07\times10^{29}\, t\exp\left(\frac{-797kJ/mol}{RT}\right)\ (T\le 1380K) \tag{7}$$

$$D_{tr} = (D_1 - D_2)\left\{Cos\left(\frac{\pi}{2}\times\frac{T-1380}{1473-1380}\right)\right\}^{(t/(3.081\times10^{-4}))} + D_2\ \ (1380K < T < 1473K) \tag{8}$$

$$D_2^{2.3} = D_0^{2.3} + 4.34\times10^{30}\, t\exp\left(\frac{-797kJ/mol}{RT}\right)\ (T\ge 1473K) \tag{9}$$

where, $D_0$ is the starting grain size and t is time.

FE Simulation of the Ring Rolling Process

Corrected flow stress data were directly used to generate the constitutive equation of FE simulation. The mathematic formula for correlating stress, strain and strain rate can be expressed as the following equation.

$$\sigma = K_0(a_0 + a_1\varepsilon)^{n_1}(b_0 + b_1\varepsilon)^{m_1} \tag{10}$$

where, $K_0$ is strength coefficient, and $n_1$ and $m_1$ are strain hardening exponent and strain rate sensitivity, respectively.

Generally, the friction between rolls and ring workpiece is expressed by the friction law of constant factor. The value of friction factor is assumed to be 0.5, and interface heat transfer coefficient between rolls and ring workpiece was applied as 11kW/m$^{2o}$C. The element used in the simulation is brick elements. Figure 3 shows the 3D modelling for rolls and initial preform (or blank) shapes. The main driving parts of ring rolling mill are composed of main roll, mandrel and axial roll. In the first step of ring rolling process, a donut-shaped blank was made by hot forming process. The blank is placed on the ring roller over an un-driven mandrel, and the mandrel is forced under pressure toward a driven main roll. The forming zones are shown schematically delineating the spread in the two passes, the radial pass by mandrel and the axial pass by axial roll. Figure 4 shows simulation results of strain and temperature distributions for ring rolling process of Alloy 783 ring. The simulation results indicate that the stain level at the

surface is higher than that at the middle area, while the temperature level at the corner of Alloy ring is lower than that at the middle area.

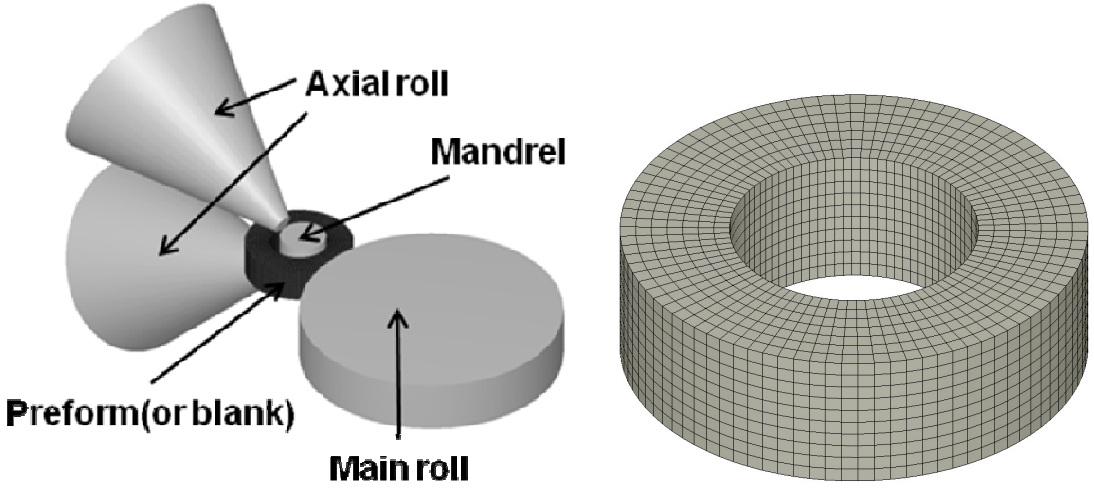


(a) (b)

Figure 3. Initial FE modelling for ring rolling process of Alloy 783: (a) ring rolling modelling at X-Y-Z plane and (b) preform modelling


(a)

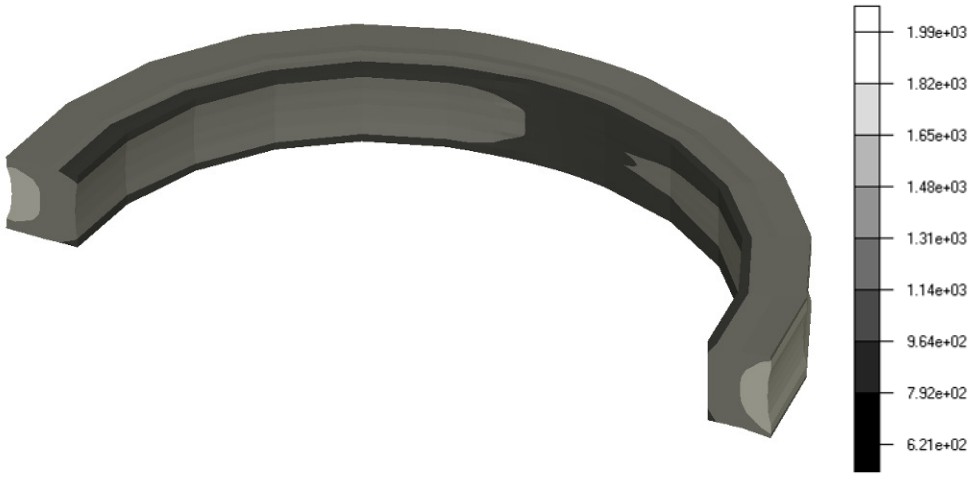


(b)

Figure 4. Contours of (a) effective strain and (b) temperature at final stage of ring-rolling process

of Alloy 783

Microstructure Prediction and Its Validation

Figure 5 shows the experimental observation of rolled Alloy 783 ring. From this figure, it can be found that the temperature at the corner of the ring is significantly decreased. This observation is in agreement with the simulation result.

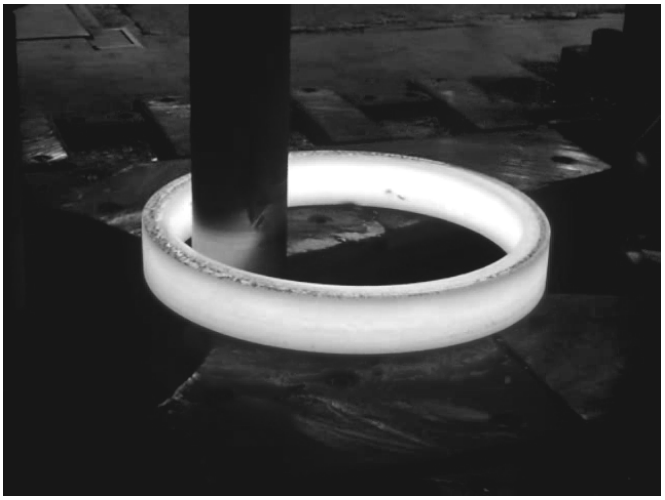

Figure 5. Ring rolled Alloy 783 ring

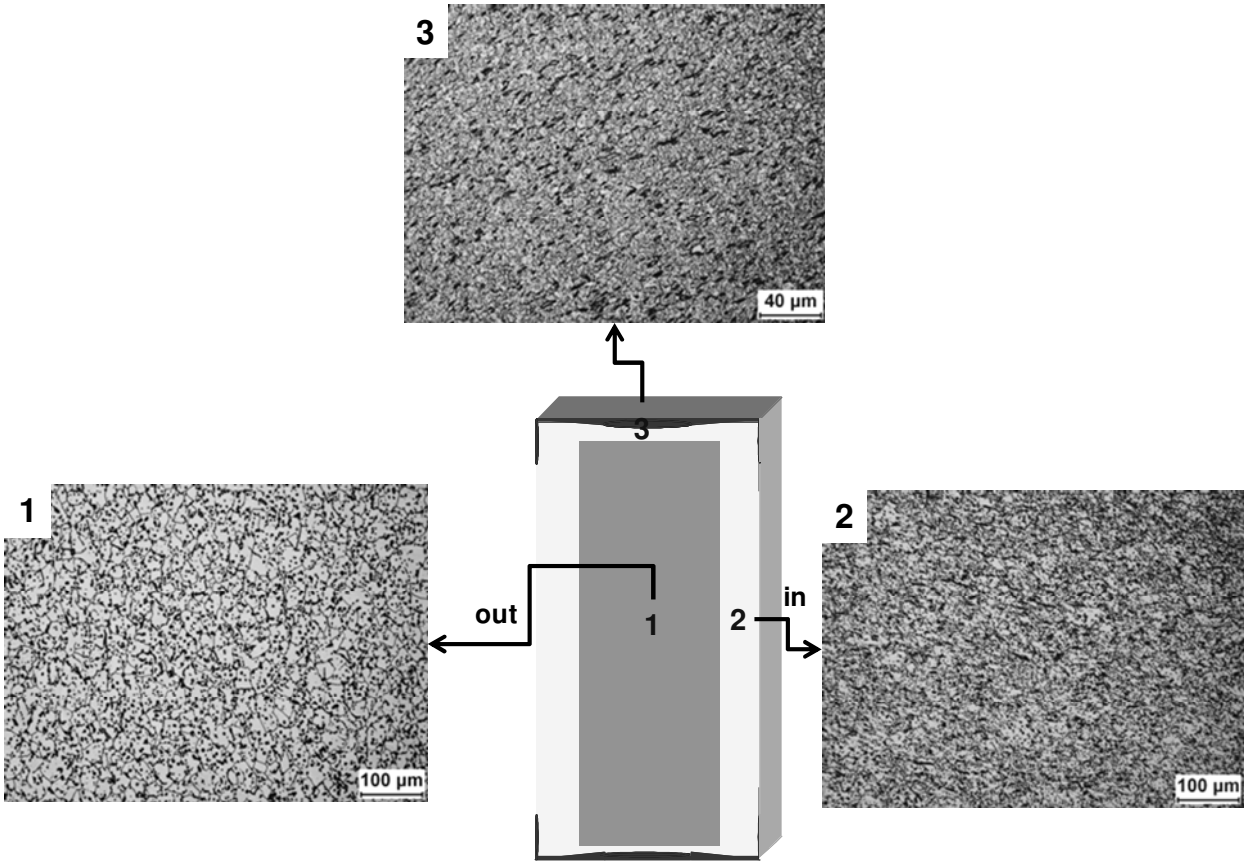


Figure 6. Microstructures observed at different locations for ring-rolled Alloy 783 ring

Figure 6 shows the microstructures observed at the cross section of the large-scale Alloy 783 ring manufactured by ring-rolling process. In the microstructural observation from the surface area to the middle area, it can be seen that the grain size at surface area is smaller than that at the middle area. This means that dynamic recrystallization is occurring at a faster rate at the surface than in the middle.

The microstructure evolution during the high temperature deformation was closely related to the internal variables such as strain, strain rate and temperature varying at different locations. In order to predict the microstructural changes at different locations during hot compression tests of Alloy 783, the de-coupled approach of the microstructure-prediction model and FE simulation was used. Firstly, the growth of the initial grain ($d_0$) during the heating and soaking was calculated by the grain growth model. After which the dynamic recrystallization model predicted the microstructure evolution of Alloy 783 during hot working. The accuracy of the microstructure-prediction model for Alloy 783 are investigated by comparing the average grain size predicted by the model and experimental data for the Alloy 783 rolled ring. In the microstructure prediction, average grain size was calculated by applying the following relation.

$$d_{av.} = \left( \frac{X_{drx}}{d_{drx}^{\,2}} + \frac{X_n}{d_0^{\,2}} \right)^{-1/2}, \quad X_n = 1 - X_{drx} \tag{11}$$

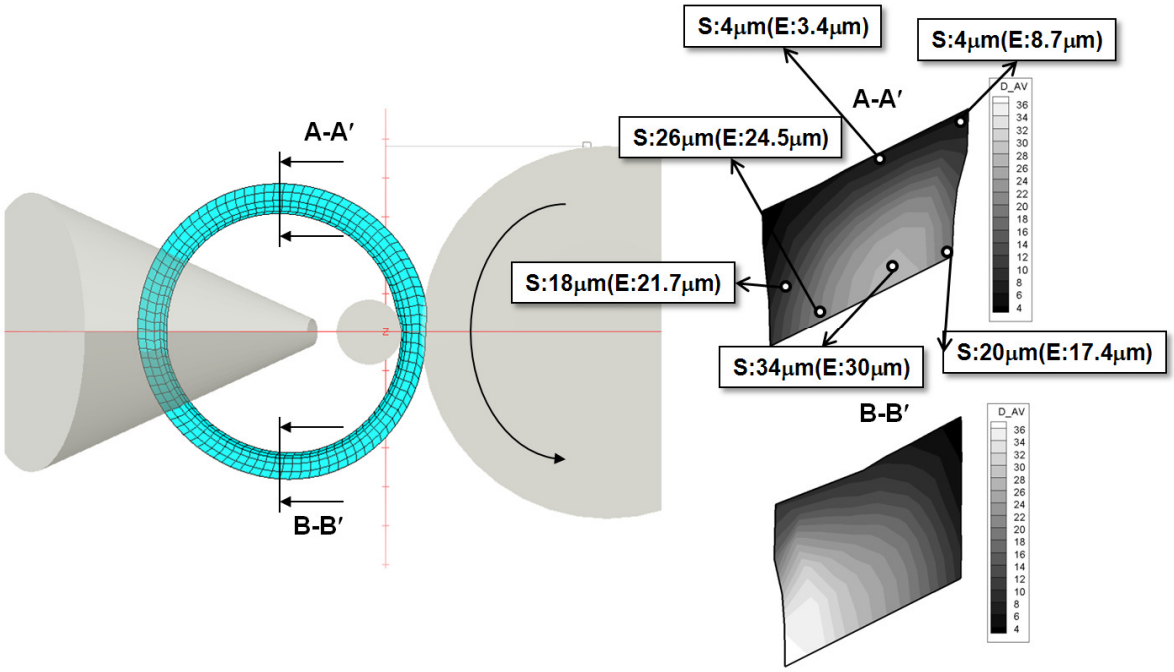


Figure 7. Contours of average grain size for Alloy 783 ring; 'S' symbol is simulation results and 'E' symbol in the bracket is measured data.

Figure 7 shows the comparison of experimental data and simulated results for average grain size of the Alloy 783 ring. The experimental data measured by actual Alloy 783 ring were over-lapped with simulation results. Especially, the values in the brackets indicate the experimental data. The simulation results at most of the positions agree well with experimental results although the average grain size measured at the upper outer corner seems to be larger than the

simulated one. The inconsistency may be due to the deviation of adiabatic heating effect between actual temperature and calculated one.
Although there is minor deviation in average grain size simulation, the present microstructure-prediction model for Alloy 783 is suggested as a useful numerical approach for the process design of high temperature deformation.

## Summary

In this work, the microstructure evolution of a large-scale Alloy ring with the outer diameter of approximately 740mm during the ring-rolling process was predicted by de-coupled approach between FE analysis and microstructure prediction model. In order to evaluate the microstructural change in Alloy 783 ring during the ring rolling process, the microstructure prediction of Alloy 783 based on dynamic recrystallization and grain growth theories was established and implemented into the post user-subroutine of a commercial FE code. In the microstructural observation from the surface area to the middle area for Alloy 783 ring, it was found that the grain size at surface area is smaller than that at the middle area. The simulation results at different locations correctly predicted these microstructural changes in the experimental observations.
Finally, the comparison of the present three dimensional FE module with the actual microstructure of ring-rolled Alloy 783 ring has successfully validated its reliability in the prediction of microstructure.

## Acknowledgments

This research was sponsored by Ministry of Knowledge Economy(MKE) and partly made by R & D project for the core industrial technology.

## References

1. J.S. Smith and K.A. Heck, “Development of a Low Thermal Expansion, Crack Growth Resistance Superalloy”, *Superalloy 1996*, ed. R.D. Kissinger et al, TMS (1996), 91-100.

2. W. Roberts and B. Ahlblom, “A Nucleation Criterion for Dynamic Recrystallization during Hot Working”, *Acta Metallurgica*, 26 (1978), 801-813.

3. J. A. Hines and K. S. Vecchio, “Recrystallization Kinetics within Adiabatic Shear Bands”, *Acta Mater.,* 45(2) (1997), 635-649.

4. F. Garofalo, “An Empirical Relation Defining the Stress Dependence of Minimum Creep Rate in Metals”, *Trans. Metall. Soc. AIME,* 227 (1963), 351-355.

5. E. I. Poliak and J. J. Jonas, “A One-Parameter Approach to Determining the Critical Conditions for the Initiation of Dynamic Recrystallization”, *Acta Mater.,* 44(1) (1996), 127-136.